Incidence angle dependency of leaf vegetation indices from hyperspectral lidar measurements

SANNA KAASALAINEN, FGI, OLLI NEVALAINEN, FGI, TEEMU HAKALA, FGI, KATI ANTTILA, FMI

Summary: We have studied the effect of incidence angle on the spectral content of leaf measurements from hyperspectral light detection and ranging (lidar) data. New results obtained for different ornamental plant leaves indicate that their backscatter properties do not follow the Lambert scattering law, especially in the visible wavelength range: specular reflections were observed near the normal incidence. Also the vegetation spectral indices, such as Normalized difference vegetation index (NDVI), or even the simple ratios may change with the laser incidence angle to the target. The reason for this is the difference in their backscatter vs. intensity behaviour between visible and near-infrared (NIR) wavelengths. In comparison with earlier results it turns out that this phenomenon seems to depend on the internal structure and surface properties of leaves. Further information on the extent and role of this effect for different leaves is needed, but our results indicate that the nature of laser reflection in tree canopies may vary between species. The calibration of hyperspectral lidar vegetation reflectance measurements must be further studied by rigorous experiments and modelling.

Zusammenfassung: (Die Abhängigkeit von Vegetationsindices für Blätter vom Inzidenzwinkel aus hyperspektralen Laserscannermessungen). In diesem Beitrag wird der Einfluss des Einfallswinkels auf spektrale Indices, welche aus hyperspektralen Laserscannermessungen von Blättern abgeleitet werden, untersucht. Neue Ergebnisse für Blätter von verschiedenen Zierpflanzen zeigen, dass deren Rückstreuverhalten vor allem in sichtbaren Bereich des elektromagnetischen Spektrums nicht dem eines Lambertschen Strahlers entspricht: bei genähert senkrechter Einfallrichtung wurde gerichtete Reflexion beobachtet. Auch spektrale Vegetationsindices wie z.B. der Normalized Difference Vegetation Index (NDVI) oder auch nur einfache Verhältnisse können sich mit dem Einfallswinkel des Laserstrahls ändern. Der Grund dafür ist ein unterschiedliches Rückstreuverhalten im sichtbaren Bereich bzw. im nahen Infrarot. Im Vergleich mit früheren Ergebnissen scheint dieses Phänomen von der inneren Struktur und den Oberflächeneigenschaften der Blätter abzuhängen. Während tiefergehende Untersuchungen zum Ausmaß und zur Rolle dieses Effekts noch ausstehen, weisen unsere Ergebnisse darauf hin, dass die Art der Laserreflexion für unterschiedliche Spezies variieren könnte. Die Kalibrierung von Reflexionsgraden aus multispektralen Laserscannermessungen erfordert weitere Studien in Hinblick auf eine strenge Modellierung und experimentelle Validierung.

1. Introduction

Photosynthetic activity in the tree canopy is a driver of growth and an indicator of tree health and productivity of plants in general. Trees with high foliar biomass and chlorophyll content have high carbon assimilation capacity. Stress induces changes in photo-synthetically-active pigments (GITELSON & MERZLYAK, 1994). Spectral indices are efficient in mapping the parameters related to vegetation health, water stress, and photosynthetic potential, because they are simple and easy to derive. (WU et al., 2008, HOUBORG & BOEGH, 2008, USTIN et al., 2009). Spectral remote sensing has been implemented at spatial resolution down to 40 cm (e.g. LAUSCH et al., 2013; KALACSKA et al., 2015). Improved resolution and more accurate 3D position for the spectra are still needed, because accurate leaf-level information on important vegetation parameters has thus far been available mainly from destructive measurements and representative sampling.

Spectral indices have traditionally been retrieved from passive spectral remote sensing (USTIN et al., 2009, LAUSCH et al., 2013, KALACSKA et al., 2015). Recently, multiwavelength terrestrial laser scanning has also been found to be a promising tool for combined structure and spectral measurement (GAULTON et al., 2013, NEVALAINEN et al., 2014, LI et al., 2014). The role of measurement geometry and the effects from laser interaction with complex structures (such as tree canopies) are not yet completely understood. The effect of the incidence angle, i.e., the angle between incoming laser beam and surface normal, on the laser scanning (intensity) data has been studied for leaves and different targets with monochromatic laser scanners, mainly for the purpose of calibrating or improving the laser scanning results (LICHTI, 2005, PESCI & TEZA, 2008, SOUDARISSANANE et al., 2011, BALDUZZI et al., 2011, KAASALAINEN et al., 2011). However, only a few studies have been carried out with multispectral or hyperspectral laser scanners. New results have emerged quite recently for dual wavelength light detection and ranging (lidar) measurements (GAULTON et al., 2013), but more information is needed on the effect of the indidence angle on spectral vegetation indices. This is partially because multispectral terrestrial laser scanners have been developed and applied only recently (DOUGLAS et al., 2012, HAKALA et al., 2012, DANSON et al., 2014, LI et al., 2014). A multispectral canopy lidar has been introduced by WOODHOUSE et al. (2012) for simultaneous retrieval of vegetation profiles and spectral indices at the canopy scale.

It has been assumed in previous studies that spectral ratios should be insensitive to the incidence angle because the backscattered intensity for each index has been measured at similar geometry. Leaves are commonly assumed to be close to Lambertian scatterers. Therefore the spectral ratios should be primarily affected by the target spectral reflectance only (GAULTON et al., 2013). In their experiment for deciduous leaves with a 4-channel multispectral lidar, SHI et al. (2013) found the influence of the incidence angle to be similar in all wavelengths for a deciduous leaf, and subsequently, no effect on a spectral ratio was observed. Conversely, EITEL et al., (2014) found the specular reflection to play an important role.

Leaf optical properties have been modelled with, e.g., the PROSPECT model from passive or simulated hyperspectral data (MORSDORF et al., 2009, WANG et al., 2015). EITEL et al. (2010, 2011) studied the relationship between foliar nitrogen and chlorophyll concentrations and laser return intensity with a green laser (532 nm) and found that the variations in leaf angles (and hence the incidence angle) complicated the predictions. ZOU et al., (2014) reported a high correlation between canopy reflectance in the red edge (at 748 nm) and leaf mean tilt angles. Thus there is a growing need for systematic experiments on the effects of leaf geometry and structure on laser return intensity and canopy reflectance in general. Especially, the role of multiple scattering and the influence of structural change on the retrieval of vegetation indices should be studied in more detail.

The main goal of this paper is to explore the effect of measurement geometry on vegetation indices retrieved with a hyperspectral lidar instrument. We study the effect of incidence angle on laser backscatter from leaves at different wavelengths and discuss the effect of the results on the future research on vegetation 3D spectral remote sensing.

2. Material and Methods

2.1 Laser scanner intensity

The radar equation defines the power (P_r) received by a laser scanner detector to be:

$$P_r = \frac{P_t D_r^2}{4\pi R^4 \beta_t^2} \sigma \qquad (1)$$

where P_t is the transmitted power, D_r is the receiver aperture, R is the range, and β_t is the transmitter beam width. σ is the backscatter cross section (HÖFLE & PFEIFER 2007), which depends on the measurement geometry as follows:

$$\sigma = \frac{4\pi}{\Omega} \rho A_s \qquad (2)$$

ρ is the reflectivity of the scatterer and Ω is the scattering solid angle. A_s is the illuminated area of the scattering element, which is a function of range R and beam width β_t:

$$A_s = \frac{\pi R^2 \beta_t^2}{4} \qquad (3)$$

Substituting this into Eq. (2), we get the backscatter cross section in the form:

$$\sigma = \pi \rho R^2 \beta_t^2 cos\alpha \qquad (4)$$

where α is the laser incidence angle to the target (SHAKER et al., 2011). In our study, all parameters, including the range R, remained constant, except for σ, which depends on the incidence angle α (cf. KAASALAINEN et al., 2011). MORSDORF et al. (2009) modelled the laser return signal from leaves with the PROSPECT model, where the leaves were assumed to be Lambertian scatterers. So the

directional component ($4\pi /\Omega$) in Eq. 2, could be neglected. This is the starting point of our study, as we can now investigate the leaf spectra at different incidence angles (α) with a hyperspectral lidar instrument.

Tab. 1: The HSL characteristics. (FWHM = Full Width at Half Maximum.)

Wavelength channels	555, 624, 691, 726, 760, 795, 899, and 1000 nm
Optical bandpass	20 nm (FWHM)
Pulse rate	5.3 kHz
Pulse length	1 ns
Average output power	41 mW
Beam diameter	4 mm at exit
Beam divergence	~0.02° at 543 nm
Range resolution	15 cm
Scan speed	Max 60°/s (vertical)

2.2 The instrument and measurements

The Hyperspectral Lidar (HSL) is a prototype multi-wavelength laser scanner with a supercontinuum laser light source (420–2400 nm). It produces a 3D point cloud with a spectrum associated to each point. A laser pulse is transmitted to a target and the range is measured from the time for the reflected pulse to return. The HSL uses a spectrograph and a 16-element avalanche photodiode (APD) array as a detector, connected to a high-speed (1ns sampling rate) 8-channel digitizer. The intensity of each transmitted laser pulse is measured and used to normalize the intensity of the backscattered laser pulse. The sensor has also been calibrated w.r.t. the measured distances separately for each wavelength. The digitizer enables data storage at 8 wavelength bands. These bands can be selected by adjusting the position of the dispersion from the spectrograph with respect to the APD array. In this study, the wavelength channels were 555, 624, 691, 726, 760, 795, 899 and 1000 nm (see Tab. 1). The rose sample was measured separately after some modifications had been made to the instrument. Therefore the channels were slightly different (cf. Sect. 2.3). A Spectralon® reference target with 99% nominal reflectance was measured at the same distance as the leaf targets. The instrument

and data processing are presented in more detail in (HAKALA et al., 2012).

The leaf samples were taken from three common ornamental plants: Chinese hibiscus (*Hibiscus rosa-sinensis*), a widely used flower in pharmacology (e.g., SHARMA & SULTANA, 2004), Zamioculcas (Common name "Zanzibar Gem") (*Zamioculcas zamiifolia*), a tropical perennial, and a rose (*Rosa* Spp.) sample commonly available in florist shops. We also scanned a sand sample taken from a beach in Kivenlahti, Finland, which was sieved into 500µm grain size. This sample has also been measured in earlier experiments with a monochromatic laser scanner, so it provided an important reference (KROOKS et al., 2013).

All measurements were carried out indoors in laboratory conditions. The leaf samples were placed on a motorized rotating platform at about 4-meter distance from the scanner. The incidence angle was changed in 5° increments, and a scan over the leaf was performed at each incidence angle.

2.3 Data processing and analysis
The measured HSL point clouds where processed using MATLAB 2013a software (The MathWorks®, Inc). Laser echoes from outside the leaf were manually removed from the point clouds. The mean backscattered reflectance of all the echoes from the leaf was used as the backscattered reflectance at each incidence angle.

The spectral indices compared in this study are commonly used in retrieveing vegetation characteristics, such as leaf chlorophyll or nitrogen content (see also NEVALAINEN et al., 2014). The chlorophyll concentration is related to plant photo-synthetic potential and senescing (GITELSON & MERZLYAK, 1994), and therefore the reliability of its measurement is crucial.

The normalized difference vegetation index (NDVI) is based on the contrast between high chlorophyll absorption at red and high reflectance (*R*) at near-infrared (TUCKER, 1979, WU et al., 2008). It has also been used for mapping leaf-area index (HOUBORG & BOEGH, 2008) and chlorophyll concentration (WU et al., 2008). The wavelength channels used in this study were 691 nm in the red and 795 nm in NIR:

$$NDVI = \frac{R_{795} - R_{691}}{R_{795} + R_{691}} \qquad (5)$$

We also compared the Red Edge Normalized Difference Vegetation Index (GITELSON & MERZLYAK, 1994), where the wavelength channels were 760 nm and 726 nm, respectively (764 and 713 for the rose).

Promising results in leaf-level chlorophyll (C_{ab}) estimation have been obtained with the so-called red edge and spectral and derivative indices such as R_{750}/R_{710} (ZARCO-TEJADA et al., 2004). This index is also called the Single Ratio or Simple Ratio (SR). A variety of wavelength combinations can be used, but we selected R_{760}/R_{726} to calculate the ratio (R_{764}/R_{713} for the rose sample).

The modified simple ratio MSR has been used to estimate chlorophyll and leaf area index (LAI) at canopy scale (WU et al., 2008).

$$MSR = \frac{R_{750}/R_{705} - 1}{\sqrt{R_{750}/R_{705}} + 1} \qquad (6)$$

In this study, we used reflectances at 760 nm and 691 nm, which were closest to those in Eq. 6, for computing the MSR (764 nm and 713 nm for the rose sample, respectively) in Eq. 6.

We also included the modified chlorophyll absorption ratio index using reflecance at 705 and 750 nm (referred here as MCARI750) and defined as follows (WU et al., 2008):

$$MCARI[705,750] = [(R_{750} - R_{705}) - 0.2 \times (R_{750} - R_{550})](\frac{R_{750}}{R_{705}}) \qquad (7)$$

In this paper, the reflectances at 760 nm, 691 nm (764 nm and 713 nm for the rose leaf sample), and 555 nm (561 for the rose) were used for the MCARI.

3. Results

3.1 Incidence angle vs. wavelength
The spectra at different incidence angles for all samples are presented in Fig. 1. The

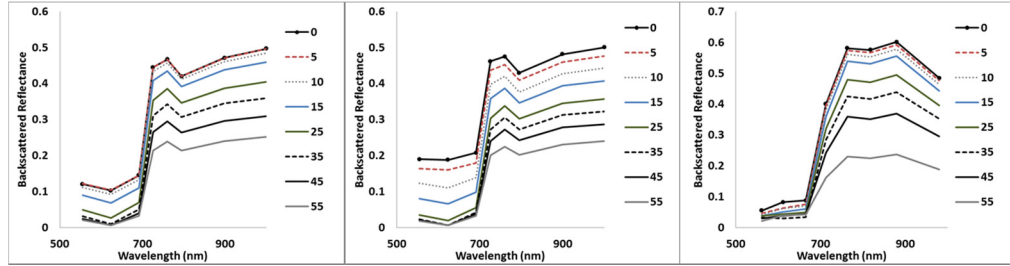spectral shape remains the same otherwise, but the decline in intensity from 0° towards

Fig. 1: Spectra vs. incidence angle. Left: Zanzibar Gem, middle: Chinese Hibiscus, right: Rose leaf.
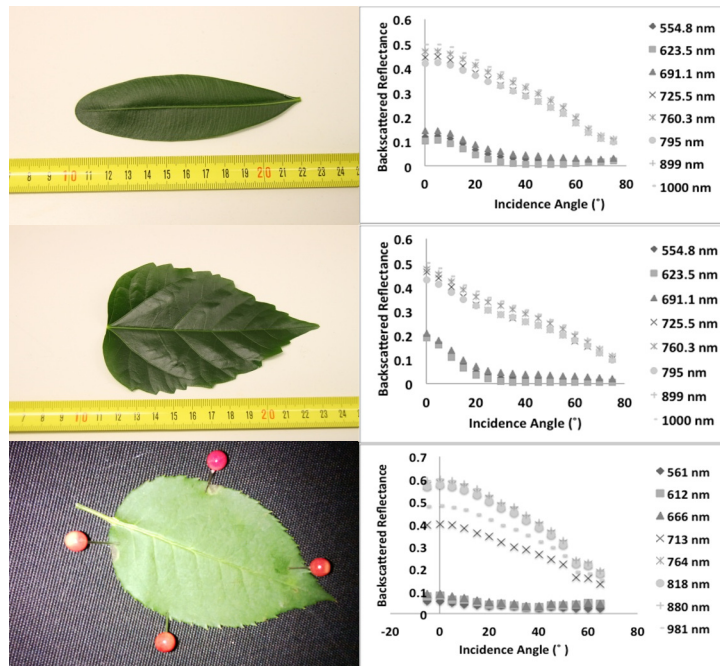

Fig. 2: The samples (left) and their incidence angle vs. backscattered reflectance (right) at all eight wavelength channels: top: Zamioculcas (Zanzibar Gem), middle: Chinese hibiscus, bottom: Rose. The pinheads are 5mm in diameter.

larger incidence angles is sharper in the visible than in the NIR spectral range. This can also be seen in the incidence angle vs. intensity curves presented in Figure 2. The intensity decline between 0° and 40° is presented in Tab. 2-3, where it can also be observed that it is prominent in the visible, but not so sharp in the NIR range. This is clearly seen in Fig. 3, where the intensities of the Zanzibar Gem sample have been normalized to 1 at 0°.

In spite of the obviously non-lambertian intensity vs. incidence behaviour in the visible range, we examined this feature a little further for the Zanzibar Gem sample, by fitting a cosine function (Eq. 4), where the term $\pi \rho R^4 \beta_t^2$ was assumed constant, as all measurements were carried out at the same distance. The results for visible (555 nm) and near-infrared (795 nm) case are shown in Fig. 4. The R^2 coefficient of determination for this fit was 0.98 (with 0.031 RMSE), which indicates a good fit in the NIR case. For 555 nm, the R^2 was 0.58, and therefore we fitted the 4th power of the cosine function (Fig. 4) to obtain a better fit

with R^2=0.99 and RMSE 0.023. It appears that at visible wavelengths the scattering does not follow the 1st order cosine function.

The Kivenlahti sand sample (Fig. 5), measured in the same experiment, showed similar incidence angle vs. intensity behaviour as in our earlier study with a monochromatic laser scanner (KROOKS et al., 2013). The decline between 0° and 40° was about 5-6% in visible and 6-8% in NIR. This means that for the sand sample, the effect of the incidence angle to the spectral shape is smaller than for the leaves.
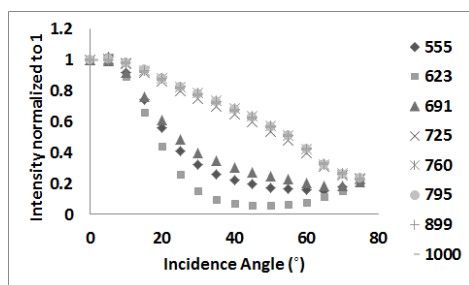

Fig. 3: Intensity normalized to 1 at 0° for the Zanzibar Gem sample.

3.2 The spectral indices
Comparison of the NDVI, simple ratio, MSR, and the MCARI[705,750] indices for all leaves are presented in Figs. 6-9. The NDVI index has also been plotted in Fig. 6 for the sand sample, to show the difference in results with those for the leaves.
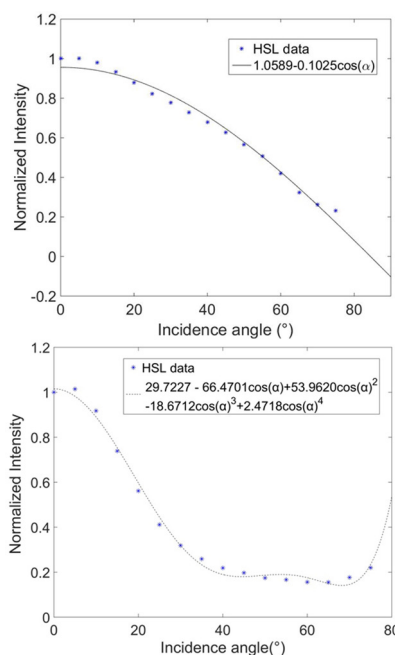

Fig. 4: Intensity normalized to 1 at 0° at 795 nm (top) and 555 nm (bottom) for the Zanzibar Gem sample (cf. Fig. 3), with the n'th order cosine function (Eq. 2, with n=1 and n=4, respectively) plotted to the data.
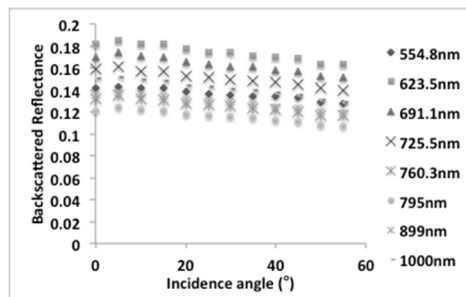

Fig. 5: Backscattered laser reflectance vs. incidence angle for beach sand, sieved into 500μm grain size.

A clear incidence angle effect is observed for all four indices, and for all leaf samples, which is not monotonic. The sharpest changes are observed at incidence angles less than 20°. The changes at incidence angles greater than 60° may be caused by inaccuracies caused by the high tilt angle of the leaves, resulting in the laser echo mixing with the surroundings. It was also found in BALDUZZI et al., (2011) that results for pear tree leaves were inaccurate at incidence

angles greater than 60°, which was also accounted for mixed intensities at high angles of incidence.
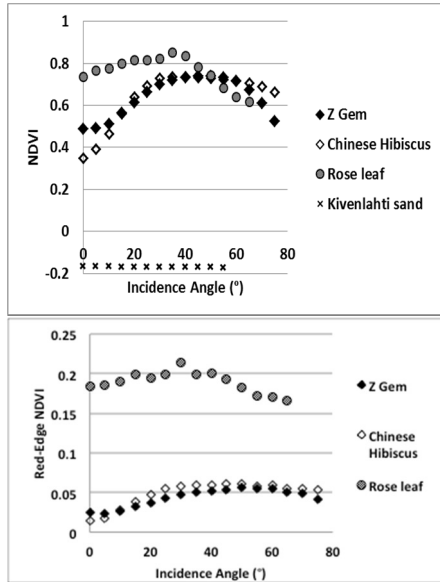

Fig. 6: Top: The NDVI index vs. incidence angle for leaf and beach sand samples. Lower: the red-edge NDVI for leaf samples.
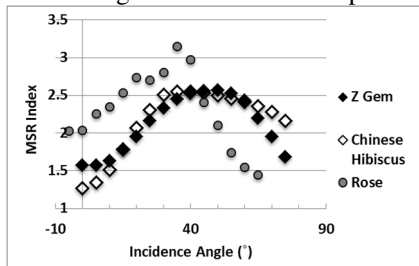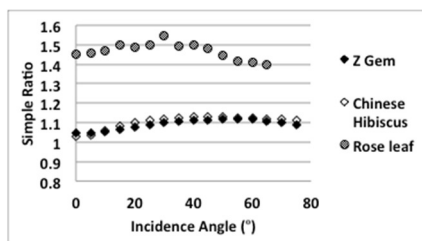

Fig. 7: The MSR index vs. incidence angle.

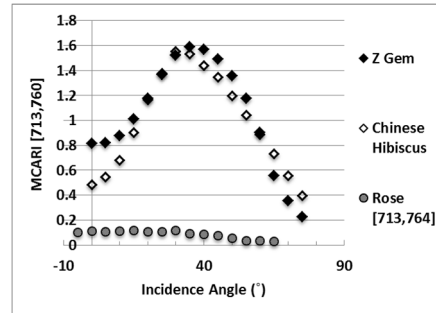**Fig. 8:** The simple ratio: R760/R726 for waxed leaves, R764/713 for the rose sample.

Fig. 9: MCARI[691,760] index for Zanzibar Gem and Chinese Hibiscus, and MCARI[713,764] for the rose leaf sample.

4. Discussion

The results are similar to those obtained by LICHTI (2005), who compared the lidar intensity vs. incidence angle in the near-infrared for different targets and observed a sharp (about 55%) decrease between 0° and 20° in the intensity of a matt black plastic. This was suggested to be due to its partially specular reflectivity, since the decrease was much less steep for other targets (such as tile). In our results, the intensity curves in Fig. 2 suggest a specular reflection, which is likely to be caused by the waxed surface of the leaf samples, especially for the Chinese hibiscus. The specular reflection is pronounced in the visible (especially red) wavelengths, where the leaf reflectance is low (Fig. 3). For the rose leaf, the specular reflection is not as prominent as for the two waxed leaf samples, but the decrease between 0° and 20° was 39% at 561 nm, while it was about 3% for the sand sample (Fig. 5).

Tab. 2: The decrease in intensity between 0° and 40° incidence angles for Zanzibar Gem at all wavelengths.

Wavelength (nm)	$I(0°)$	$I(40°)$	Drop in %
555	0.12	0.03	78
624	0.10	0.007	93
691	0.14	0.04	70
726	0.44	0.29	35
760	0.47	0.32	32
795	0.42	0.29	32
899	0.47	0.32	32
1000	0.50	0.33	33

Tab. 3: As in Tab. 2, for Chinese Hibiscus.

Wavelength	$I(0°)$	$I(40°)$	Drop in %

Wavelength (nm)			
555	0.19	0.02	89
624	0.19	0.006	97
691	0.21	0.04	81
726	0.46	0.26	47
760	0.47	0.32	39
795	0.43	0.26	40
899	0.48	0.29	39
1000	0.50	0.30	40

Tab. 4: As in Tab. 2, for Rose.

Wavelength (nm)	$I (0°)$	$I (40°)$	Drop in %
561	0.05	0.03	53
612	0.08	0.03	65
666	0.08	0.03	61
713	0.40	0.26	34
764	0.58	0.39	32
818	0.58	0.38	33
880	0.60	0.41	32
981	0.48	0.32	33

No signs of specular reflection were found for an oriental plane (*Platanus orientalis*) leaf sample by SHI et al. (2013). The results obtained by BALDUZZI et al., (2011) for conference pear (*Pyrus Commmunis*) tree leaves at 785 nm did not show any strong specular reflection either. This result is similar to ours at NIR wavelengths, but more leaf types with different surface properties and internal structure should be studied to understand the role of specular reflection in the visible part of the spectrum. Also, the influence of the laser footprint size should be investigated, as the beam divergence is known to increase with increasing wavelength. We carried out the distance calibration separately at each wavelength to reduce the effect of laser spot size.

Although these results are preliminary, they confirm the role of laser incidence to the target and laser reflection in the canopy that must be taken into account when measuring vegetation indices with laser scanning.

In a 3D measurement over a large and complex target, such as a tree, there are multiple echoes resulting from laser hits to more than one leaf/needle. The leaf curvature, angular distribution, and other shape irregularities are likely to average the effect of incidence angle, at least in the tree scale. This, however, must be better characterized in future experiments, particularly in the spectral red edge and NIR spectral regions.

5. Conclusion

We have studied vegetation spectral indices with hyperspectral laser scanning and found that they change with the laser incidence angle to the target.

These results call for an extensive study of multispectral laser vegetation indices to get a better understanding of their sensitivity to variations in the leaf angle distribution. In the future, hyperspectral laser scanning will enable the retrieval of quantitative 3D/4D distributions of plant eco-physiological variables from vegetation indices. A better understanding of scattering effects on vegetation indices would improve the reliability of the measurement, so that the indices can be accurately mapped over an entire tree instead of sampling individual leaves.

Future research will include more leaf types and varying measurement geometries. More information on the role of measurement geometry in laser scanning of vegetation canopies can then be obtained by modelling the leaf-laser interaction with a leaf scattering model (such as the PROSPECT), effects of shoot and canopy structure on laser backscatter, and including a large set of leaf/needle types. The leaf scattering models also need to be upgraded to simulate specular reflectance.

Acknowledgements

References

BALDUZZI, M. A. F., VAN DER ZANDE, D., STUCKENS, J., VERSTRAETEN, W. W. & COPPIN, P., 2011: The Properties of Terrestrial Laser System Intensity for Measuring Leaf Geometries: A Case Study with Conference Pear Trees (*Pyrus Communis*). - Sensors **11** (12): 1657–1681.

DANSON, F. M., GAULTON, R., ARMITAGE, R. P., DISNEY, M., GUNAWAN, O., LEWIS, P. & RAMIREZ, A. F. (2014): Developing a dual-

wavelength full-waveform terrestrial laser scanner to characterize forest canopy structure. – Agricultural and Forest Meteorology **198-199**: 7–14.

Douglas, E. S., Strahler, A., Martel, J., Cook, T., Mendillo, C., Marshall, R., Chakrabarti, S., Schaaf, C., Woodcock, C., Li, Z., Yang, X., Culvenor, D., Jupp, D., Newnham, G. & Lovell, J. 2012: DWEL: A Dual-Wavelength Echidna Lidar for ground-based forest scanning. - IEEE IGARSS, 4998–5001.

Eitel, J. U. H., Vierling, L. A., Long, D. S. & Hunt, E. R., 2011: Early season remote sensing of wheat nitrogen status using a green scanning laser. – Agricultural and Forest Meteorology **151** (10): 1338–1345.

Eitel, J. U. H., Vierling, L. A. & Long, D. S., 2010: Simultaneous measurements of plant structure and chlorophyll content in broadleaf saplings with a terrestrial laser scanner. – Remote Sensing of Environment **114** (10): 2229–2237.

Eitel, J. U. H., Magney, T. S., Vierling, L. A. & Dittmar, G., 2014: Assessment of crop foliar nitrogen using a novel dual-wavelength laser system and implications for conducting laser-based plant physiology. – ISPRS Journal of Photogrammetry and Remote Sensing **97**: 229–240.

Gaulton, R., Danson, F. M., Ramirez, F. A. & Gunawan, O., 2013: The potential of dual-wavelength laser scanning for estimating vegetation moisture content. – Remote Sensing of Environment **132**: 32–39.

Gitelson, A. & Merzlyak, M. N., 1994: Spectral Reflectance Changes Associated with Autumn Senes- cence of Aesculus hippocastanum L. and Acer platanoides L. Leaves. Spectral Features and Relation to Chlorophyll Estimation. – Journal of Plant Physiology **143** (3) 286– 292.

Hakala, T., Suomalainen, J., Kaasalainen, S. & Chen, Y. 2012: Full waveform hyperspectral LiDAR for terrestrial laser scanning. – Optics Express **20** (7): 7119-7127.

Houborg, R. & Boegh, E. 2008: Mapping leaf chlorophyll and leaf area index using inverse and forward canopy reflectance modeling and SPOT reflectance data. – Remote Sensing of Environment **112** (1): 186–202.

Höfle, B. & Pfeifer, N. 2007: Correction of laser scanning intensity data: Data and model-driven approaches. – ISPRS Journal of Photogrammetry and Remote Sensing **62** (6): 415–433.

Kaasalainen, S., Jaakkola, A., Kaasalainen, M., Krooks, A. & Kukko, A. 2011: Analysis of

Incidence Angle and Distance Effects on Terrestrial Laser Scanner Intensity: Search for Correction Methods. – Remote Sensing **3** (12): 2207–2221.

Kalacska, M., Lalonde, M., & Moore, T. R. 2015. Estimation of foliar chlorophyll and nitrogen content in an ombrotrophic bog from hyperspectral data: scaling from leaf to image. – Remote Sensing of Environment **169**, 270-279.

Krooks, A., Kaasalainen, S., Hakala, T. & Nevalainen, O., 2013: Correction of Intensity Incidence Angle Effect in Terrestrial Laser Scanning, – ISPRS Annals of the Photogrammetry, Remote Sensing and Spatial Information Sciences **II-5** (W2): 145-150.

Lausch, A., Heurich, M., Gordalla, D., Dobner, H.-J., Gwillym-Margianto, S. & Salbach, C. 2013: Forecasting potential bark beetle outbreaks based on spruce forest vitality using hyperspectral remote-sensing techniques at different scales. – Forest Ecology and Management 308, 76–89.

Li, W., Sun, G., Niu, Z., Gao, S. & Qiao, H. 2014: Estimation of leaf biochemical content using a novel hyperspectral full-waveform LiDAR system. – Remote Sensing Letters **5** (8): 693–702.

Lichti, D. D. 2005: Spectral Filtering and Classification of Terrestrial Laser Scanner Point Clouds. – The Photogrammetric Record **20** (111): 218–240.

Morsdorf, F., Nichol, C., Malthus, T. & Woodhouse, I. H. 2009: Assessing forest structural and physiological information content of multi-spectral LiDAR waveforms by radiative transfer modelling. – Remote Sensing of Environment **113** (10): 2152–2163.

Nevalainen, O., Hakala, T., Suomalainen, J., Mäkipää, R., Peltoniemi, M., Krooks, A. & Kaasalainen, S. 2014: Fast and nondestructive method for leaf level chlorophyll estimation using hyperspectral LiDAR. – Agricultural and Forest Meteorology 198-199: 250–258.

Pesci, A. & Teza, G. 2009: Effects of surface irregularities on intensity data from laser scanning: an experimental approach. – Annals of Geophysics **51** (5-6): 839-848.

Shaker, A., Yan, W. Y. & El-Ashmawy, N. 2011: The effects of laser reflection angle on adiometric correction of the airborne lidar intensity data. – The International Archives of the Photogrammetry, Remote Sensing and Spatial Information Sciences **38** (5/W12): 213-217.

Sharma, S. & Sultana, S. 2004: Effect of Hibiscus rosa sinensis Extract on Hyperproliferation and Oxidative Damage

Caused by Benzoyl Peroxide and Ultraviolet Radiations in Mouse Skin. – Basic & Clinical Pharmacology & Toxicology **95** (5): 220–225.

SHI, S., SONG, S., GONG, W., DU, L., ZHU, B. & HUANG, X. 2015: Improving Backscatter Intensity Calibration for Multispectral LiDAR. – IEEE Geoscience and Remote Sensing Letters, **12** (7): 1421–1425.

SOUDARISSANANE, S., LINDENBERGH, R., MENENTI, M. & TEUNISSEN, P. 2011: Scanning geometry: Influencing factor on the quality of terrestrial laser scanning points. – ISPRS Journal of Photogrammetry and Remote Sensing **66** (4): 389–399.

TUCKER, C. J., 1979: Red and Photographic Infrared Linear Combinations for Monitoring Vegetation, Remote Sensing of Environment, **8** (2): 127-150.

USTIN, S. L., ROBERTS, D. A., GAMON, J. A., ASNER, G. P. & GREEN, R. O. 2004: Using Imaging Spectroscopy to Study Ecosystem Processes and Properties. – BioScience **54** (6): 523-534.

WANG, Z., SKIDMORE, A. K., WANG, T., DARVISHZADEH, R. & HEARNE, J. 2015: Applicability of the PROSPECT model for estimating protein and cellulose+lignin in fresh leaves. – Remote Sensing of Environment **168:** 205–218.

WOODHOUSE, I. H., NICHOL, C., SINCLAIR, P., JACK, J., MORSDORF, F., MALTHUS, T. J. & PATENAUDE, G. 2011: A Multispectral Canopy LiDAR Demonstrator Project. – IEEE Geoscience and Remote Sensing Letters **8** (5): 839–843.

WU, C., NIU, Z., TANG, Q, & HUANG, W. 2008: Estimating chlorophyll content from hyperspectral vegetation indices: Modeling and validation. – Agricultural and Forest Meteorology **148** (8-9): 1230–1241.

ZARCO-TEJADA, P., MILLER, J. ., MORALES, A., BERJÓN, A. & AGÜERA, J. 2004: Hyperspectral indices and model simulation for chlorophyll estimation in open-canopy tree crops. – Remote Sensing of Environment **90** (4): 463–476.

ZOU, X., MÕTTUS, M., TAMMEORG, P., TORRES, C. L., TAKALA, T., PISEK, J., MÄKELÄ, P., STODDARD, F. L. & PELLIKKA, P. 2014: Photographic measurement of leaf angles in field crops. – Agricultural and Forest Meteorology, **184**: 137–146.

Address of the Authors:

DR. SANNA KAASALAINEN, OLLI NEVALAINEN, TEEMU HAKALA, Finnish Geospatial Research Institute – FGI, Masala, Finland. Tel +358-50-3696806, e-mail: sanna.kaasalainen@nls.fi, olli.nevalainen@nls.fi, teemu.hakala@nls.fi

KATI ANTTILA, Finnish Meteorological Institute (FMI), Helsinki, Finland. Tel.: +358-50-4412298, e-mail: kati.anttila@fmi